



# Findings of suspicious calcifications on contrast-enhanced mammography and their pathological correlation

Dilşah Oral<sup>1</sup>  
 İhsan Şebnem Örgüç<sup>1</sup>  
 Hanife Seda Mavili<sup>2</sup>  
 Teoman Coşkun<sup>3</sup>

<sup>1</sup>Manisa Celal Bayar University Hafsa Sultan Hospital,  
Department of Radiology, Manisa, Türkiye

<sup>2</sup>Manisa Celal Bayar University Hafsa Sultan Hospital,  
Department of Pathology, Manisa, Türkiye

<sup>3</sup>Manisa Celal Bayar University Hafsa Sultan Hospital,  
Department of General Surgery, Manisa, Türkiye

## PURPOSE

This study aimed to determine the performance of contrast-enhanced mammography (CEM) in evaluating suspicious calcifications not associated with a mass.

## METHODS

Patients with suspicious calcifications detected on CEM performed at our center between February 2021 and December 2023 were included in the study. Retrospectively, the morphology, distribution, and longest axis length of the calcifications were assessed on low-energy images, whereas contrast enhancement intensity, pattern, longest axis length, and enhancement curves were analyzed on recombined images. The pathological diagnosis, grade, Ki-67 index, and (if available) the longest lesion length in the surgical specimen were recorded. Using pathology as the gold standard, various CEM parameters were evaluated for their performance in assessing this group of calcifications. Primary and secondary analyses were performed based on combined low or no enhancement and no enhancement alone, respectively.

## RESULTS

Our study includes 132 lesions in 114 patients, 18 of whom had bilateral calcifications. Of the 132 lesions included in the study, 78 were benign, and 54 were malignant. Sensitivity, specificity, positive predictive value, and negative predictive value were determined as follows: 72.2%, 62.8%, 57.3%, and 76% in low-energy images; 79.6%, 80.8%, 74.1%, and 85.1% in the primary analysis of recombined images; and 98.2%, 47.4%, 56.4%, and 97.4% in the secondary analysis. Contrast enhancement intensity was identified as a significant parameter influencing malignancy risk. A strong statistical correlation was observed between lesion length measurements in both low-energy and recombined images compared with pathology ( $r = 0.733$  and  $r = 0.879$ ,  $P < 0.001$  for both), with mean differences of  $-4.75$  mm and  $+4.45$  mm. No statistically significant relationship was found between contrast enhancement intensity and the distinction between invasive and *in situ* carcinoma ( $P = 0.698$ ) or the differentiation of ductal carcinoma *in situ* grade ( $P = 0.336$ ). A significant correlation was detected between pathology and dynamic contrast enhancement types adapted from magnetic resonance imaging (MRI) ( $P = 0.019$ ). Although no statistically significant linear correlation was found between the Ki-67 index and contrast enhancement intensity, the  $P$  value was close to significance ( $P = 0.057$ ).

## CONCLUSION

CEM demonstrates strong performance in the assessment of suspicious calcifications by combining the morphological and distributional features of digital mammography with enhancement characteristics similar to MRI.

## CLINICAL SIGNIFICANCE

The findings support that CEM exhibits effective performance in evaluating suspicious calcifications not associated with a mass and may have a potential role in routine clinical practice.

## KEYWORDS

Contrast-enhanced mammography, suspicious calcifications, breast cancer

Corresponding author: Dilşah Oral

E-mail: dilsahoral@gmail.com

Received 17 March 2025; revision requested 13 April 2025; accepted 12 June 2025.



Epub: 21.07.2025

Publication date:

DOI: 10.4274/dir.2025.253352

**B**reast cancer is the most common cancer among women, and mammography is the primary screening method.<sup>1</sup> Calcifications are frequently observed findings on mammograms.<sup>2</sup> According to the Breast Imaging Reporting and Data System (BI-RADS) atlas, based on their morphology and distribution, calcifications are typically classified as benign or suspicious.<sup>3</sup> Some suspicious calcifications may represent invasive cancer or ductal carcinoma *in situ* (DCIS), the earliest stage of breast cancer. Approximately one-third of breast cancers present solely as calcifications on mammography.<sup>4</sup> Histopathological sampling is recommended for BI-RADS 4 and BI-RADS 5 calcifications.<sup>3</sup>

In the diagnosis of breast cancer, ultrasonography (USG) and magnetic resonance imaging (MRI), which are used in addition to mammography, detect calcifications at a low rate or may not detect them at all. In recent years, contrast-enhanced mammography (CEM) has become increasingly utilized as an imaging technique that, comparable with MRI, demonstrates neovascularization in the breast through the use of iodinated contrast agents. In malignant lesions, vascular structures formed during angiogenesis exhibit increased permeability, allowing intravenously administered contrast agents to penetrate the tumor, resulting in enhancement.<sup>5,6</sup> In CEM, two image types are acquired: low-energy and high-energy. Low-energy images are considered equivalent to digital mammography and are suitable for the evaluation of calcifications.<sup>7</sup> Recombined images, generated using both low- and high-energy images, demonstrate enhancement. In CEM, although the morphology and distribution of calcifications are assessed in low-energy images, the functional characteristics of the same tissue can also be evaluated using recombined images.

#### Main points

- Contrast-enhanced mammography (CEM) is an imaging technique based on the dual-energy method and provides information on tissue function in addition to the structural evaluation of calcifications.
- According to our study, the presence of enhancement in the calcification region exhibited a sensitivity of 98.2% for malignancy.
- Recombined images demonstrating enhancement provided more accurate results in determining tumor length compared with low-energy mammographic equivalent images. This suggests that CEM may reduce the positive surgical margin rate in calcifications.

Our study aims to investigate the utility of CEM, a relatively new and increasingly adopted technique, in the characterization of suspicious calcifications not associated with a mass. Additionally, we aim to evaluate our hypothesis that CEM may help reduce unnecessary biopsies, contribute to determining the extent of disease in patients undergoing breast-conserving surgery, and decrease the rate of positive surgical margins.

## Methods

Approval was obtained from Manisa Celal Bayar University Clinical Research Ethics Committee for this retrospective study (decision number: 20.478.486/2230, date: 31/01/2024). Between February 2021 and December 2023, CEM images of 910 patients with clinically suspected malignancy and/or suspicious findings detected by other imaging modalities were reviewed. Patients with suspicious calcifications not associated with a mass were selected. Patients without suspicious calcifications, those with suspicious calcifications associated with a mass, those with suspicious calcifications but accompanied by a mass in another focus, and those who had received neoadjuvant therapy before imaging were excluded from the study. With 96 patients having lesions (calcification focus) in a single breast and 18 patients having lesions in both breasts, in 114 patients a total of 132 lesions were included in this retrospective study (Figure 1).

### Contrast-enhanced mammography examinations

All lesions included in this study were imaged using a digital mammography system

with dual-energy capability (Pristina, GE, Rue De La Minière, Buc, France) available in the clinic. A low-osmolar, nonionic contrast agent (Opaxol 350 mg/mL, Kopaq 350 mg/mL) was administered at a dose of 1.5 mL/kg, with a maximum volume of 100 mL, using an automatic injector system (Medrad) at a rate of 3 mL/s. Imaging commenced 1.5–2 minutes after the start of contrast injection. Craniocaudal and mediolateral oblique (MLO) images were acquired in both breasts, starting with the target breast. Additionally, in cases suspicious for malignancy, around the 8<sup>th</sup> minute, a second MLO image (delayed phase) of the pathological breast was obtained after the MLO image of the non-target breast. The total procedure lasted approximately 8–9 minutes, depending on patient compliance. Low-energy images were acquired at 28–32 kVp, and high-energy images were obtained at 45–49 kVp. The filtration material and kVp values were automatically determined by the system. Recombined images were automatically generated from the low- and high-energy images.

### Image analysis

The images were evaluated in consensus by two observers: one radiologist with 34 years of experience in breast imaging and a fourth-year radiology resident. During the assessment of the CEM images, the BI-RADS CEM lexicon published by the American College of Radiology in 2022 was used. Suspicious calcifications were classified based on their morphology and distribution using the low-energy images, which are equivalent to standard mammography. According to the BI-RADS atlas, calcifications with a morphol-

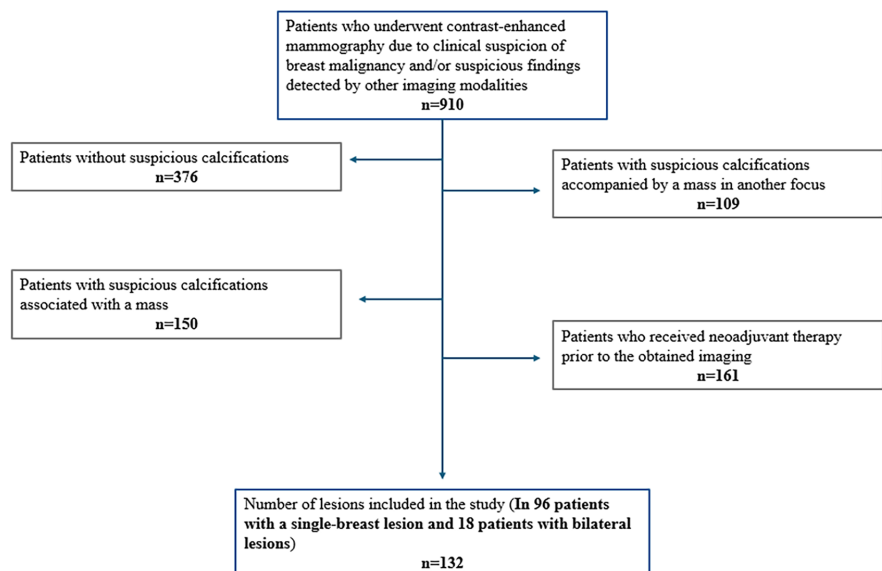


Figure 1. Flowchart of the study.

ogy or distribution associated with <50% malignancy were categorized as low-suspicion (amorphous, coarse heterogeneous, fine pleomorphic and diffuse, regional, grouped), and those associated with ≥50% malignancy were classified as high-suspicion (fine linear/fine linear branching and linear, segmental). Cases were categorized into three risk groups: low-risk if both morphology and distribution were low-suspicion, intermediate-risk if one was high-suspicion, and high-risk if both were high-suspicion. In the analysis of low-energy images, the low-risk group was considered benign, whereas the intermediate- and high-risk groups were classified as malignant. On the recombined images, the relationship between the suspicious calcification area and the enhancing tissue was assessed in four categories: no enhancement observed, partial enhancement of the tissue, complete enhancement with overlapping characteristics, or enhancement extending beyond the calcification area. The enhancement pattern was classified as homogeneous, heterogeneous, or clumped. The intensity of enhancement was qualitatively graded as high, moderate, low, or absent. If delayed-phase images were available, the enhancement intensity was compared qualitatively between the early and delayed phases, and inspired by the dynamic contrast enhancement curves used in MRI, enhancement patterns were classified as type 1 (persistent) if there was an increase between the two phases, type 2 (plateau) if the signal remained stable, and type 3 (washout) if there was a decrease. The longest length of the calcifications and enhancing area was measured in a single plane using the projection where they appeared largest. For patients who did not undergo pathological sampling and/or were placed under follow-up, particularly those in whom the level of suspicion was lowered based on other imaging modalities (USG or MRI) and who declined histopathological sampling, prior and follow-up examinations were reviewed for dimensional changes. Cases classified as benign were required to demonstrate stability for ≥2 years.

Pathological analysis

The pathology reports of patients who underwent sampling were reviewed, and detailed pathological diagnosis was recorded. All sampled patients underwent tru-cut biopsy, and surgical specimen data were also available for a subset of these patients. The histopathological grades of *in situ* lesions were documented. In cases with surgical specimens, the longest tumor dimension

and pathological diagnosis were included in the dataset. Additionally, the Ki-67 index was recorded for invasive carcinomas.

Statistical analysis

Statistical analyses were conducted using IBM Corp., Armonk, NY, USA SPSS Statistics version 27.0. Frequency tables and descriptive statistics were used for data interpretation. Parametric methods were applied for measurement values that followed a normal distribution. Specifically, analysis of variance (F-test) was used to compare measurement values among three or more independent groups, whereas the paired sample t-test (t-value) was used for comparisons between two dependent groups. For measurement values that did not follow a normal distribution, non-parametric methods were applied. In this context, the Wilcoxon test (Z-value) was used to compare two dependent groups. The Pearson chi-squared ( $\chi^2$ ) test was employed to assess relationships between two categorical variables. For correlations between two normally distributed quantitative variables, Pearson correlation and Bland–Altman plots were used, whereas Spearman's correlation coefficient was applied if at least one variable did not follow a normal distribution. To determine

risk factors influencing malignancy risk, binary logistic regression analysis using the backward likelihood ratio model was performed. A *P* value of <0.05 was considered indicative of a statistically significant relationship.

Results

The study included a total of 132 lesions. All 114 patients were women (age range, 25–79 years, average 48.4 years). A total of 36 lesions were considered benign due to their stability for at least 2 years and the absence of additional malignant features. A total of 42 lesions were pathologically benign, and 54 were malignant. Among the malignant lesions, 25 were invasive carcinomas, and 29 were *in situ* (Table 1).

In low-energy images, where morphology and distribution were evaluated together, sensitivity was found to be 72.2%, specificity 62.8%, positive predictive value (PPV) 57.3%, negative predictive value (NPV) 76.5%, and accuracy 66.7%; 23.4% of the low-, 52.5% of the intermediate-, and 88.9% of the high-risk group were malignant.

In the evaluation based on contrast enhancement intensity in recombined images, of the lesions without contrast enhance-

Table 1. Pathological distributions		
	n	Total
Pathologically malignant		
Invasive ductal carcinoma	22	54
Invasive lobular carcinoma	3	
Ductal carcinoma <i>in situ</i>	27	
Lobular carcinoma <i>in situ</i>	2	
Pathologically benign		
Benign with atypia		42
Atypical ductal hyperplasia	3	
Flat epithelial atypia	1	
Apocrine atypia	1	
Benign without atypia		
Papilloma	4	
Fibrocystic changes	4	
Fat necrosis	3	
Fibroadenomatous changes	2	
Ductal hyperplasia without atypia	9	
Apocrine metaplasia	4	
Adenosis	5	
Non-specific connective tissue	2	
Inflammatory process	3	
Ductal ectasia	1	
Classified as benign		36
		132

ment, 97.4% (37/38) were benign. In cases with low contrast enhancement, 72.2% (26/36) were benign. As an example, Figure 2 illustrates this finding. In contrast, moderate and high enhancement intensities were more frequently associated with malignancy, with 61.9% (13/21) and 81.1% (30/37) of the lesions being malignant, respectively. Among the non-enhancing lesions, only one was malignant. In the primary analysis, where non-enhancing and low-intensity enhancing lesions were grouped as benign and moderate and high-intensity enhancing lesions were grouped as malignant, a statistically significant relationship was found between pathology and contrast enhancement intensity categories ( $P < 0.001$ ). In the secondary analysis, where non-enhancing lesions were classified as benign and any degree of contrast enhancement was classified as malignant, a statistically significant relationship was found between the categories ( $P < 0.001$ ) (Table 2).

In the primary analysis, the sensitivity was 79.6%, specificity was 80.8%, PPV was 74.1%, NPV was 85.1%, and accuracy was 80.3%. In the secondary analysis, the sensitivity increased to 98.2%, but the specificity decreased to 47.4%. The PPV was 56.4%, NPV was 97.4%, and accuracy was 68.2%. In the receiver operating characteristics analysis, the area under the curve (AUC) for low-energy images was 0.67, whereas the AUC for recombined images was 0.80 in the primary analysis and 0.73 in the secondary analysis (Figure 3). According to regression analysis, malignancy risk is 14 times higher for low-, 60 times for moderate-, and 159 times for high-intensity contrast than for non-enhancing lesions.

In the analysis evaluating the relationship between contrast enhancement intensity and invasiveness, 25 lesions (46.3%) were invasive, and 29 (53.7%) were *in situ* carcinoma. No statistically significant association was found between these two parameters ( $P = 0.698$ ). Of the 29 *in situ* carcinomas, 2 were lobular carcinoma *in situ* and 27 were DCIS. All but one DCIS showed enhancement. Among the 26 DCIS lesions, 5 were low-grade (2 low, 2 moderate, 1 high enhancement intensity), 9 intermediate-grade (1 low, 4 moderate, 4 high enhancement intensity), and 12 high-grade (2 low, 2 moderate, 8 high enhancement intensity). No statistically significant association was found between the histopathological grade of DCIS and contrast enhancement intensity ( $P = 0.336$ ).

Out of 132 lesions, 17 (12.9%) exhibited a homogeneous contrast enhancement pattern (10 benign, 7 malignant), 70 (53%) showed a heterogeneous pattern (25 benign,

45 malignant), and 7 (5.3%) demonstrated a clumped pattern (6 benign, 1 malignant). In 38 lesions (28.8%), no contrast enhancement was observed. Among the 54 malig-

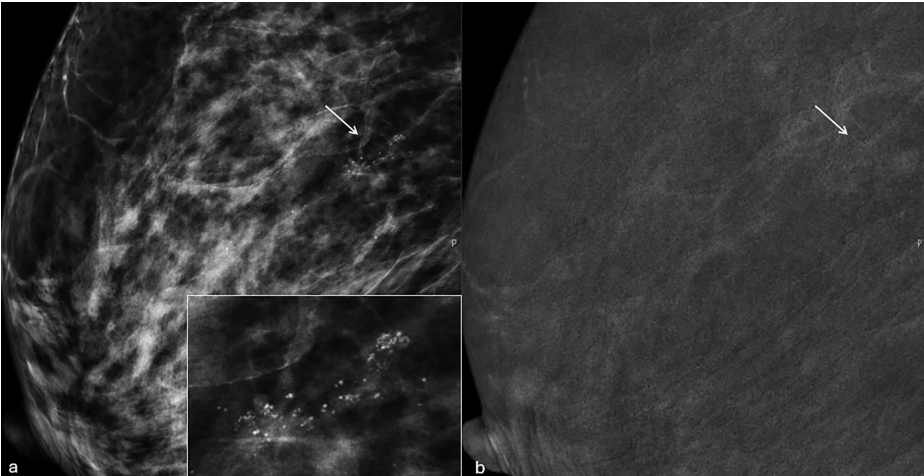


**Figure 2.** In the low-energy mediolateral oblique image (a) of a 53-year-old female patient, suspicious calcifications with a fine pleomorphic morphology and linear distribution are observed. In the recombined image (b), low-intensity enhancement extending beyond the calcification site is noted. The pathological diagnosis was benign.

Table 2. Primary and secondary analyses of contrast enhancement intensities and pathological outcomes					
Contrast enhancement intensity	Benign (n = 78)		Malignant (n = 54)		Pearson's chi-squared ( $\chi^2$ ) test <i>P</i> value
	n	%	n	%	
Primary analysis					
Favoring benign (no + low enhancement)	63	80.8	11	20.4	$\chi^2 = 47,256$ <i>P</i> < 0.001
Favoring malignancy (moderate + high enhancement)	15	19.2	43	79.6	
Secondary analysis					
Favoring benign (no enhancement)	37	47.4	1	1.9	$\chi^2 = 32,343$ <i>P</i> < 0.001
Favoring malignancy (all types of enhancement)	41	52.6	53	98.1	
Pearson's chi-squared ( $\chi^2$ ) test with cross-tabulations was used to evaluate the association between two categorical variables.					

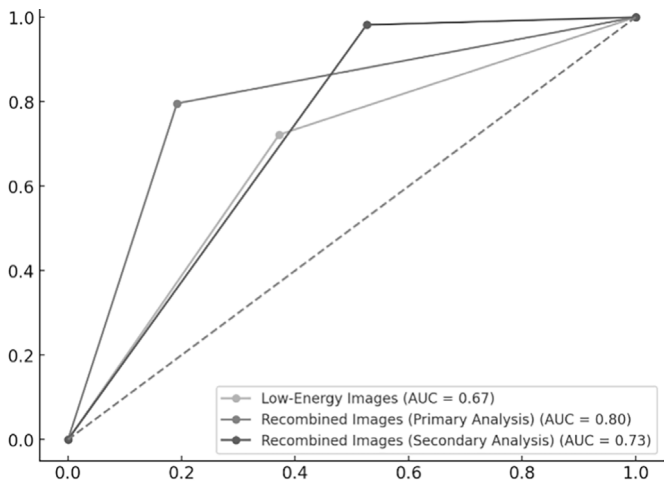


**Figure 3.** Receiver operating characteristic curves for both images and analyses. AUC, area under the curve.



nant lesions, 83% exhibited heterogeneous enhancement, whereas only 13% showed homogeneous enhancement. The statistical analysis yielded  $P = 0.018$ , indicating that heterogeneous contrast enhancement is significantly associated with malignancy.

In 22 cases (16.6%), partial contrast enhancement was observed in the calcification region, and in another 22 cases (16.6%), enhancement completely overlapped with this tissue. In 50 cases (37.9%), contrast enhancement extended beyond the calcified tissue. Among the 21 lesions that underwent excision in the center and did not receive neoadjuvant therapy before surgery, with surgical specimen data, 13 showed enhancement extending beyond the calcification, 4 had partial enhancement, and 3 exhibited complete overlap. One non-enhancing case was excluded. Figure 4 presents a malignant case with contrast enhancement extending beyond the calcifications; in this case, the lesion length measured on the recombined image closely matched the pathological excision size. Correlation analysis revealed a strong and statistically significant relationship between lesion length in both low-energy ( $r = 0.733$ ,  $P < 0.001$ ) and recombined images ( $r = 0.879$ ,  $P < 0.001$ ) and pathological length. The Wilcoxon signed-rank test revealed no statistically significant difference between the methods (Table 3). Bland–Altman analysis showed that recombined images tend to overestimate lesion length by 4.45 mm, whereas low-energy images tend to underestimate it by 4.75 mm (Figure 5).

In the 13 patients who exhibited contrast enhancement extending beyond the calcifications and constituted the majority of the pathologically sampled group, correlation analysis showed a strong positive and statistically significant relationship between pathological length and both calcification ( $r = 0.822$ ,  $P < 0.001$ ) and contrast-enhanced area length ( $r = 0.825$ ,  $P < 0.001$ ), similar to the overall group. This group was important for addressing the question of whether the pathological extent exceeded what was observed on low-energy images. The paired sample test revealed a significant difference between pathological and calcification length ( $P = 0.012$ ), indicating that calcification length alone may underestimate the true extent of the lesion.

In the analysis of dynamic contrast-enhancement types, 8 lesions were excluded due to the absence of late-phase images, and 28 lesions were excluded due to a lack of contrast enhancement. Among the 46 benign lesions, 38 (82.6%) exhibited a type 1 enhancement.

Among the 50 malignant lesions, 28 (56%) showed a type 1, 16 (32%) exhibited a type 2, and 6 (12%) demonstrated a type 3. Figure 6 presents a case demonstrating high-intensity contrast enhancement with a type 1 dynamic enhancement pattern, which was ultimately diagnosed as benign. The majority of lesions with type 2 (72.7%) and type 3 (75%) enhancement were malignant. Figure 7 illustrates an example of type 3 contrast enhancement with a washout pattern, corresponding to a malignant case. A statistically significant association was found between type and malignancy/benignity ( $P = 0.019$ ).

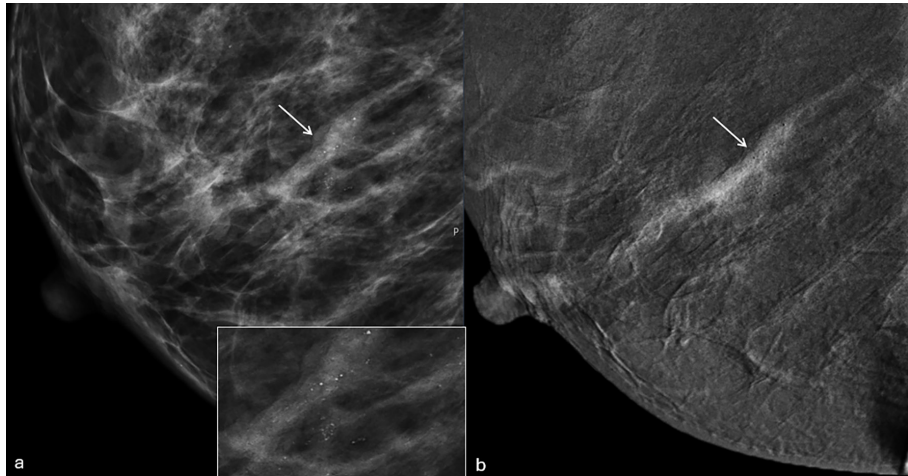


**Figure 4.** In the low-energy mediolateral oblique image (a) of a 42-year-old female patient, suspicious calcifications with a fine pleomorphic morphology and segmental distribution are observed. In the recombined image (b), high-intensity heterogeneous enhancement extends beyond the calcification site, reaching the nipple. The pathological diagnosis was ductal carcinoma *in situ*, and the measured pathological length closely matched the lesion length observed in the recombined images.

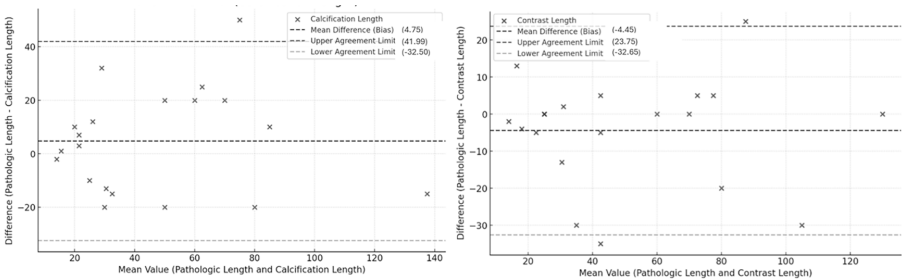


**Figure 5.** Bland–Altman plots visualizing the discrepancies between the pathological and imaging length. The left one shows results for low-energy images, and the right one is for recombined images.

	Length (mm)		Wilcoxon signed-rank test $P$ value	Spearman's $\rho$ (rho) $P$ value
		Median (IQR)		
Pathological length	49.15 $\pm$ 33.22	36.0 (50.5)		
Microcalcification length	44.40 $\pm$ 32.31	40.0 (39.0)	$Z = -0.880$ $P = 0.379$	$r = 0.733$ $P < 0.001$
Enhancement length	53.60 $\pm$ 33.39	47.5 (48.8)	$Z = 1.084$ $P = 0.278$	$r = 0.879$ $P < 0.001$

The Wilcoxon signed-rank test was used to assess paired differences between measurements. Spearman's correlation coefficient ( $\rho$ ) was calculated to evaluate the relationship between imaging and pathological sizes. IQR, interquartile range; SD, standard deviation.

However, no statistically significant association was found between enhancement types and the distinction between invasive and *in situ* carcinoma ( $P = 0.331$ ) (Table 4).

In the 25 invasive carcinoma cases with available Ki-67 index data, no statistically significant linear relationship was found between Ki-67 (%) values and contrast enhancement intensity ( $P = 0.057$ ). The median (interquartile range) Ki-67 values were 20.0 (12.3), 8.5 (19.5), and 45.0 (60.0) for lesions with low-, moderate-, and high-intensity enhancement, respectively.

## Discussion

In the analysis of groups categorized based on morphology and distribution, the findings indicate that although low-energy images (i.e., mammography) demonstrate good performance according to our classification, they may still lead to missed malignancy in 23.4% of patients with low-suspicion features. Therefore, according to the BI-RADS atlas, pathological sampling is recommended, even for patients we classified as having low suspicion. However, this approach resulted in unnecessary biopsy recommendations in 47.5% of the intermediate suspicion group and 11.1% of the high suspicion group. These findings on standard mammography support the need for functional assessment of the tissue using CEM, an alternative imaging modality.

Our study identified only one malignant case that did not exhibit contrast enhancement that was diagnosed as intermediate-grade DCIS. We attributed the absence of enhancement to the *in situ* nature and a low Ki-67 of only 1%. As the contrast enhancement intensity increased, the malignancy rate was observed to rise across groups. In the secondary analysis, a much higher sensitivity was achieved than with the primary analysis and low-energy images. If contrast enhancement presence alone is considered a malignancy indicator, CEM achieves 98.2% sensitivity, almost eliminating the risk of missing malignant cases. However, in the secondary analysis, specificity decreased, leading to a higher false-positive rate. On the other hand, the increase in NPV indicates that in the absence of enhancement, CEM can rule out malignancy with 97.4% accuracy. The primary analysis provided a more balanced and consistent performance, albeit with slightly lower sensitivity. From a breast cancer diagnostic perspective, missing a diagnosis can have fatal consequences, so avoiding false negatives should be prioritized. Although false positives may lead to unnecessary biopsies, the high NPV suggests that some unnecessary procedures can be avoided. Low-intensity contrast enhancement may have been confused with background enhancement in some cases, potentially affecting our findings. Additionally, the qualitative nature of our study presents another limitation: the lack of sharply defined classification boundaries.

Among various studies, where the presence of enhancement is considered a malignant feature, our secondary analysis demonstrated the highest sensitivity and NPV.<sup>8-11</sup>

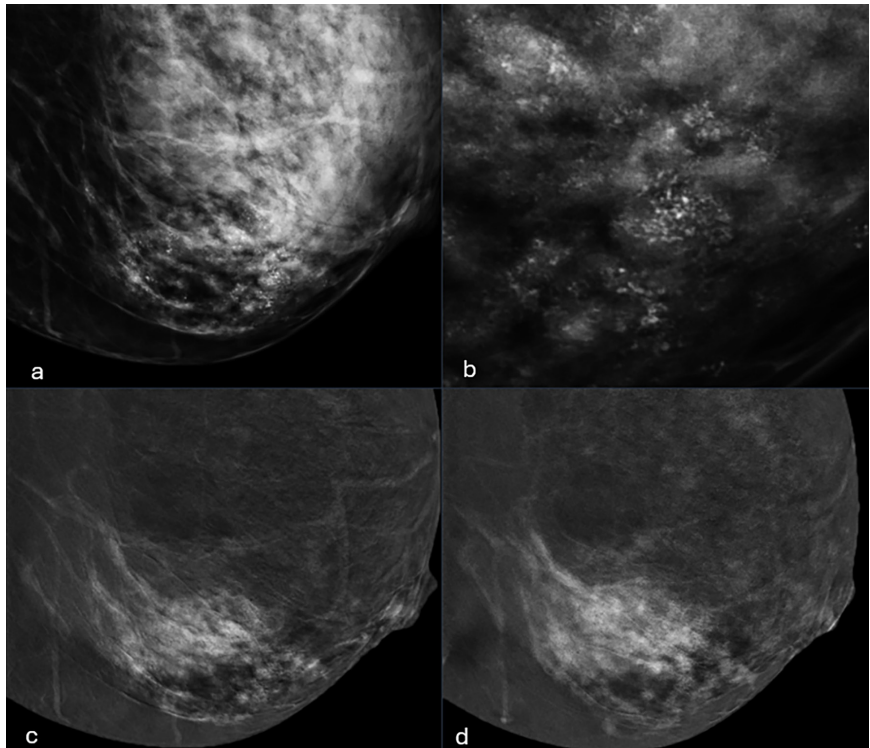


**Figure 6.** In the low-energy mediolateral oblique (MLO) image of a 44-year-old female patient (a) and the corresponding magnified view (b), suspicious calcifications with coarse heterogeneous morphology and segmental distribution are observed. In the recombined early-phase (c) and recombined delayed-phase (d) MLO images, heterogeneous, high-intensity contrast enhancement overlapping the calcification area is noted, with an increase in intensity from the early to the delayed phase, consistent with a type 1 (persistent) enhancement pattern. The pathological diagnosis was papillomatous changes with benign characteristics.

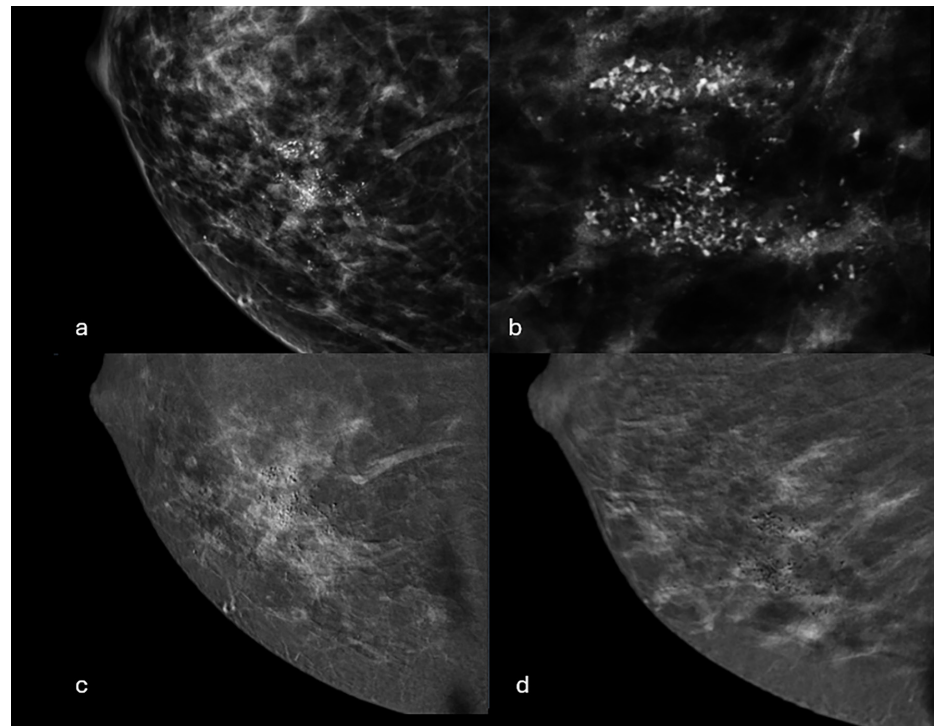


**Figure 7.** In the low-energy mediolateral oblique (MLO) image (a) and its magnified view (b) of a 48-year-old female patient, suspicious calcifications with a coarse heterogeneous morphology and grouped distribution are observed. In the recombined early-phase MLO image (c) and late-phase MLO image (d), high-intensity heterogeneous enhancement extending beyond the calcification site is noted, with more intense enhancement in the early phase, followed by a decrease in the late phase, which was a type 3 (washout) pattern. The pathological diagnosis was intermediate-grade ductal carcinoma *in situ*.

**Table 4.** Distribution of dynamic enhancement types in benign and malignant and invasive and *in situ* Lesions

Dynamic enhancement type	Benign (n = 46)		Malignant (n = 50)		Pearson's chi-squared ( $\chi^2$ ) test P value
	n	%	n	%	
1	38	82.6	28	56.0	$\chi^2 = 7.907$ <b>P = 0.019</b>
2	6	13	16	32.0	
3	2	4.4	6	12.0	
	Invasive malignant (n = 24)		<i>In situ</i> malignant (n = 26)		
	n	%	n	%	
1	11	45.8	17	65.4	$\chi^2 = 2.210$ <b>P = 0.331</b>
2	10	41.7	6	23.1	
3	3	12.5	3	11.5	

Pearson's chi-squared ( $\chi^2$ ) test with cross-tabulations was used to evaluate the association between two categorical variables.

In the majority of studies, NPV was consistently found to be high. This supports the role of CEM as a valuable imaging tool in reducing unnecessary biopsies for suspicious calcifications, which are relatively more challenging to sample than mass lesions.

In the study by Nicosia et al.<sup>11</sup>, a primary analysis similar to ours was also conducted. Their findings reported a sensitivity of 53.3%, specificity of 95.8%, PPV of 84.2%, NPV of 82.9%, and an accuracy of 83.2%. Similar to our study, in the secondary analysis, sensitivity increased but specificity decreased. In another study among 24 cases, all malignant lesions exhibited contrast enhancement at varying intensities. All *in situ* carcinomas and one benign lesion showed low-intensity enhancement, whereas the remaining benign lesions showed no enhancement.<sup>12</sup> Quantitative studies that include various breast lesions, rather than being specific to suspicious calcifications, have also identified a trend of lower contrast enhancement intensity in benign lesions and higher in malignant lesions.<sup>13-17</sup>

In studies evaluating suspicious calcifications not associated with a mass with MRI, a 2016 meta-analysis reported that studies assessing the presence of enhancement found MRI to have an average sensitivity of 92%, specificity of 75%, PPV of 78%, and NPV of 93%.<sup>18</sup> In a study by Taskin et al.<sup>19</sup>, which included 444 cases of suspicious calcifications detected on mammography, MRI demonstrated a sensitivity of 95.2%, specificity of 40.2%, PPV of 49.2%, and NPV of 93.3%. These findings are highly comparable with our secondary analysis. The effectiveness of MRI in assessing tissue function is undeniable, but the primary advantage of CEM over MRI is its ability to overlay functional infor-

mation directly onto the low-energy image, which already provides a detailed assessment of calcification morphology and distribution. MRI does not visualize calcifications and only allows for the interpretation of tissue function. As a result, evaluation requires additional digital mammography, necessitating the integration of two separate imaging modalities. Moreover, differences in patient positioning—prone for MRI and upright for mammography—can make three-dimensional localization and anatomical correlation between calcifications and enhancement more challenging. Additionally, MRI's longer acquisition time, limited accessibility, lower patient tolerance, and high cost further highlight the need for an alternative imaging method in this patient group.<sup>20</sup>

In the comparison of both images, the sensitivity, NPV, accuracy, and AUC of recombined images alone were found to be higher than those of low-energy images in both analyses. Although these values were compared separately in our study, CEM inherently combines both imaging types. Therefore, it can be anticipated that assessing findings together would significantly enhance the overall diagnostic performance.

Studies in the literature evaluating specifically suspicious calcifications have typically assessed the distinction between invasive and *in situ* carcinoma or the grading of DCIS based solely on the presence or absence of contrast enhancement.<sup>9,10,21,22</sup> In our study, however, all but 1 malignant lesion exhibited contrast enhancement. In one study including 15 lesions, all DCIS cases exhibited low contrast enhancement; however, the variation in enhancement intensity among invasive ductal carcinoma cases introduces inconsistency, limiting its reliability in clearly

differentiating these two entities.<sup>12</sup> Our results suggest that there is a predominance of high-intensity contrast enhancement in invasive carcinomas; however, since half of the *in situ* cases also exhibited high-intensity enhancement, this prevented us from obtaining a statistically significant distinction. Similarly, although no statistically significant relationship was found between contrast enhancement intensity and the histopathological grade of DCIS, 66.6% of high-grade cases demonstrated high-intensity enhancement. Although the relationship was not statistically significant, a trend toward higher enhancement in high-grade lesions was observed. Larger-scale studies are needed to obtain more definitive conclusions.

When evaluating contrast enhancement patterns, it was observed that heterogeneous enhancement was more prominent in malignant cases, whereas more than half of the homogeneously enhancing lesions were benign. These results are consistent with the existing literature.<sup>16,17</sup> Clumped enhancement did not provide meaningful data due to the limited number of cases in this group.

Recombined images outperformed low-energy images, exhibiting a smaller mean difference and a higher correlation coefficient. The group with contrast enhancement extending beyond the calcification area was particularly important in evaluating our hypothesis: "Could the pathological tissue be larger than what is observed in low-energy images?" In this subgroup, the correlation coefficient for recombined images was higher than for low-energy images, indicating a stronger association. Additionally, a statistically significant difference was observed between low-energy images and pathological length. In the study by Cheung et al.<sup>8</sup>, low-energy images overestimated pathological length by an average of 4.2 mm, whereas recombined images showed a smaller mean difference of 0.5 mm, indicating a more accurate length estimation. However, Houben et al.<sup>9</sup> reported a mean difference of 0.3 mm for low-energy and 4.5 mm for recombined images, although the correlation coefficients in their study were comparable with those in our study. To our knowledge, there is no other study specifically comparing the lesion length between CEM and pathology in this group. Most of the studies mentioned above, as well as other studies including various breast lesions in the literature, share a common finding: contrast-enhanced images tend to overestimate lesion length, which is consistent with our study's results.<sup>12,23-25</sup> In some studies, the



mean difference between pathology and low-energy images was smaller, but in all cases, recombined images exhibited a higher correlation coefficient, indicating a stronger association between recombined images and pathological length. The overestimation in CEM can be attributed to contrast agent extravasation into the surrounding tissue due to increased vascular permeability and compression applied during imaging, which may further disperse tissues and enhance lesion dimensions. Some studies have identified that low-energy images may also overestimate lesion length, which could be attributed to breast compression.<sup>8,9,23</sup> However, contrary to this, in our study, low-energy images tended to underestimate lesion length. This finding supports our hypothesis that relying solely on mammographic images in breast-conserving surgery may increase the risk of positive surgical margins.

To our knowledge, no prior study has specifically analyzed dynamic enhancement patterns in suspicious calcifications without a mass. A significant association was found between enhancement types and malignancy. Compared with a previous study that evaluated various breast lesions, the main difference in our findings is that approximately half of our malignant lesions also exhibited a type 1 enhancement.<sup>15</sup> We attribute this difference to the higher metabolic activity of mass-forming lesions in previous studies compared with the suspicious calcifications not associated with a mass in our study, which may result in faster contrast uptake and washout kinetics.

The other parameter we evaluated was the Ki-67 index, a marker of tumor cell proliferation, which has been associated with higher relapse rates and lower survival.<sup>26</sup> In recent years, the potential impact of pre-treatment prognosis prediction on therapy selection has led to increasing interest in assessing whether Ki-67 levels—and consequently prognosis—can be inferred from imaging findings. To our knowledge, the only two studies in the literature investigating CEM and Ki-67 were conducted by Depretto et al.<sup>27</sup> Their findings showed that most non-enhancing lesions had a Ki-67 index <20%, whereas more than half of the malignant, contrast-enhancing calcifications had a Ki-67 index >20%.<sup>10</sup> In our study, only invasive carcinomas were analyzed. Although the median Ki-67 index in moderately enhancing lesions was unexpectedly lower than in low-enhancing lesions, disrupting a clear linear relationship, the *P* value was very close

to statistical significance (0.05). The high-intensity enhancement group had the highest median Ki-67 values. Although answering the question of whether higher contrast enhancement at diagnosis could indirectly indicate a worse prognostic factor requires larger studies with broader patient populations, our findings suggest promising potential for further investigation in this area.

Our study was conducted retrospectively, which presents certain limitations. Some benign lesions were considered benign without histopathological confirmation. Even if stability is observed over a 2-year period, considering such lesions as benign—particularly in cases of *in situ* carcinomas, which may progress slowly—may not be a controversial approach in clinical practice. Retrospective evaluation reveals that in the majority of these patients, the suspicion of malignancy was significantly reduced through additional imaging methods and clinical experience, and the decision for follow-up without biopsy was made in accordance with patient preference. Additionally, surgical tumor length data of some patients were not available. For comparisons with pathology, only the longest dimension in a single imaging plane was used. Other measurements in our study were qualitative. Furthermore, this was a single-center study, which may limit the generalizability of the findings.

In conclusion, CEM offers a significant advantage over MRI in the evaluation of suspicious calcifications, as it allows for the simultaneous assessment of both calcification morphology and distribution as well as tissue functionality. This dual capability, which combines the mammographic equivalent low-energy images with MRI-like recombined images, enhances diagnostic accuracy beyond mammography alone and provides valuable insights into tumor extent, potentially aiding surgical decision-making. Through various analyses, we found that the presence of enhancement demonstrated high sensitivity for malignancy, and increasing enhancement intensity correlated with a higher malignancy risk. Additionally, CEM outperformed mammography alone in detecting malignancy and could assist in surgical planning by better reflecting disease extent. However, despite its potential, contrast enhancement intensity did not achieve statistical significance for distinguishing invasive from *in situ* carcinoma or for grading DCIS. Dynamic time-intensity analysis, similar to MRI kinetics, may aid lesion characterization, and the potential role of en-

hancement intensity as a prognostic factor warrants further investigation. Given the limited number of studies focusing on this subgroup, larger-scale, multicenter research is needed for more robust conclusions. CEM remains a promising imaging modality for suspicious calcifications, a category where radiologists have yet to reach a consensus on standard practice, routine approaches vary, and pathological sampling remains relatively challenging. It has the potential to provide more reliable and clinically useful results, making it a valuable candidate for wider implementation.

## Footnotes

### Conflict of interest disclosure

The authors declared no conflicts of interest.

## References

1. Sung H, Ferlay J, Siegel RL, et al. Global Cancer Statistics 2020: GLOBOCAN Global Cancer Statistics 2020: GLOBOCAN estimates of incidence and mortality worldwide for 36 cancers in 185 countries. *CA Cancer J Clin*. 2021;71(3):209-249. [\[Crossref\]](#)
2. Lorena Arancibia Hernández P, Taub Estrada T, López Pizarro A, Lorena Díaz Cisternas Carla Sáez Tapia M. Breast calcifications: description and classification according to BI-RADS 5<sup>th</sup> edition. Published online 2016. [\[Crossref\]](#)
3. Sickles E, D'Orsi CJ, Bassett LW, et al. ACR BI-RADS® Mammography. In: ACR BI-RADS® Atlas, Breast Imaging Reporting and Data System. Reston, VA: American College of Radiology; 2013. [\[Crossref\]](#)
4. Horvat JV, Keating DM, Rodrigues-Duarte H, Morris EA, Mango VL. Calcifications at digital breast tomosynthesis: imaging features and biopsy techniques. *RadioGraphics*. 2019;39(2):307-318. [\[Crossref\]](#)
5. Patel BK, Lobbes MBI, Lewin J. Contrast enhanced spectral mammography: a review. *Semin Ultrasound CT MR*. 2018;39(1):70-79. [\[Crossref\]](#)
6. Kuhl C. The current status of breast MR imaging Part I. Choice of technique, image interpretation, diagnostic accuracy, and transfer to clinical practice. *Radiology*. 2007;244(2):356-378. [\[Crossref\]](#)
7. Lalji UC, Jeukens CRLPN, Houben I, et al. Evaluation of low-energy contrast-enhanced spectral mammography images by comparing them to full-field digital mammography using EUREF image quality criteria. *Eur Radiol*. 2015;25(10):2813-2820. [\[Crossref\]](#)
8. Cheung YC, Tsai HP, Lo YF, Ueng SH, Huang PC, Chen SC. Clinical utility of dual-energy contrast-enhanced spectral mammography



- for breast microcalcifications without associated mass: a preliminary analysis. *Eur Radiol.* 2016;26(4):1082-1089. [\[Crossref\]](#)
9. Houben IP, Vanwetswinkel S, Kalia V, et al. Contrast-enhanced spectral mammography in the evaluation of breast suspicious calcifications: diagnostic accuracy and impact on surgical management. *Acta Radiol.* 2019;60(9):1110-1117. [\[Crossref\]](#)
  10. Depretto C, D'Ascoli E, Della Pepa G, et al. Assessing the malignancy of suspicious breast microcalcifications: the role of contrast enhanced mammography. *Radiol Med.* 2024;129(6):855-863. [\[Crossref\]](#)
  11. Nicosia L, Bozzini AC, Signorelli G, et al. Contrast-enhanced spectral mammography in the evaluation of breast microcalcifications: controversies and diagnostic management. *Healthcare.* 2023;11(4):511. [\[Crossref\]](#)
  12. Łuczyńska E, Niemiec J, Hendrick E, et al. Degree of enhancement on contrast enhanced spectral mammography (CESM) and Lesion type on mammography (MG): comparison based on histological results. *Med Sci Monit.* 2016;22:3886-3893. [\[Crossref\]](#)
  13. Rudnicki W, Heinze S, Piegza T, Pawlak M, Kojs Z, Łuczyńska E. Correlation between enhancement intensity in contrast enhancement spectral mammography and types of kinetic curves in magnetic resonance imaging. *Med Sci Monit.* 2020;26:920742. [\[Crossref\]](#)
  14. Rudnicki W, Heinze S, Niemiec J, et al. Correlation between quantitative assessment of contrast enhancement in contrast-enhanced spectral mammography (CESM) and histopathology-preliminary results. *Eur Radiol.* 2019;29(11):6220-6226. [\[Crossref\]](#)
  15. Deng CY, Juan YH, Cheung YC, et al. Quantitative analysis of enhanced malignant and benign lesions on contrast-enhanced spectral mammography. *Br J Radiol.* 2018;91(1086). [\[Crossref\]](#)
  16. Mohamed Kamal R, Hussien Helal M, Wessam R, Mahmoud Mansour S, Godda I, Alieldin N. Contrast-enhanced spectral mammography: Impact of the qualitative morphology descriptors on the diagnosis of breast lesions. *Eur J Radiol.* 2015;84(6):1049-1055. [\[Crossref\]](#)
  17. Chi X, Zhang L, Xing D, Gong P, Chen Q, Lv Y. Diagnostic value of the enhancement intensity and enhancement pattern of CESM to benign and malignant breast lesions. *Medicine.* 2020;99(37):e22097. [\[Crossref\]](#)
  18. Bennani-Baiti B, Baltzer PA. MR Imaging for diagnosis of malignancy in mammographic microcalcifications: a systematic review and meta-analysis. *Radiology.* 2017;283(3):692-701. [\[Crossref\]](#)
  19. Taskin F, Kalayci CB, Tuncbilek N, et al. The value of MRI contrast enhancement in biopsy decision of suspicious mammographic microcalcifications: a prospective multicenter study. *Eur Radiol.* 2021;31(3):1718-1726. [\[Crossref\]](#)
  20. Hobbs MM, Taylor DB, Buzynski S, Peake RE. Contrast-enhanced spectral mammography (CESM) and contrast enhanced MRI (CEMRI): patient preferences and tolerance. *J Med Imaging Radiat Oncol.* 2015;59(3):300-305. [\[Crossref\]](#)
  21. Cheung YC, Juan YH, Lin YC, et al. Dual-energy contrast-enhanced spectral mammography: enhancement analysis on BI-RADS 4 non-mass microcalcifications in screened women. *PLoS One.* 2016;11(9):0162740. [\[Crossref\]](#)
  22. Shetat OMM, Moustafa AFI, Zaitoon S, Fahim MII, Mohamed G, Gomaa MM. Added value of contrast-enhanced spectral mammogram in assessment of suspicious microcalcification and grading of DCIS. *Egypt J Radiol Nucl Med.* 2021;52(1):186. [\[Crossref\]](#)
  23. Luczyńska E, Heinze-Paluchowska S, Dyczek S, Blecharz P, Rys J, Reinfuss M. Contrast-enhanced spectral mammography: comparison with conventional mammography and histopathology in 152 women. *Korean J Radiol.* 2014;15(6):689-696. [\[Crossref\]](#)
  24. Patel BK, Garza SA, Eversman S, Lopez-Alvarez Y, Kosiorek H, Pockaj BA. Assessing tumor extent on contrast-enhanced spectral mammography versus full-field digital mammography and ultrasound. *Clin Imaging.* 2017;46:78-84. [\[Crossref\]](#)
  25. Fallenberg EM, Dromain C, Diekmann F, et al. Contrast-enhanced spectral mammography: does mammography provide additional clinical benefits or can some radiation exposure be avoided? *Breast Cancer Res Treat.* 2014;146(2):371-381. [\[Crossref\]](#)
  26. Petrelli F, Viale G, Cabiddu M, Barni S. Prognostic value of different cut-off levels of Ki-67 in breast cancer: a systematic review and meta-analysis of 64,196 patients. *Breast Cancer Res Treat.* 2015;153(3):477-491. [\[Crossref\]](#)
  27. Depretto C, Borelli A, Liguori A, et al. Contrast-enhanced mammography in the evaluation of breast calcifications: preliminary experience. *Tumori.* 2020;106(6):491-496. [\[Crossref\]](#)